



the negative active material is graphite (C<sub>6</sub>), the electrolyte is LiPF<sub>6</sub> solution (3:7 EC/EMC solvent), and the positive active material is lithium-ion phosphate (LFP)[13]. The model assumes that the electrode active material consists of ideal spherical particles of uniform size, regardless of the electric double layer effect, the reaction occurs only at the electrode/electrolyte interface, and no secondary reactions occur in the reaction process, and no gas is generated [14]. The 18650 lithium-ion battery has a multi-layer winding structure [15]. The one-dimensional electrochemical component simplifies the battery into a linear structure on the model according to the main moving direction of lithium ions during the actual charging process of the battery, as shown in Figure 1.

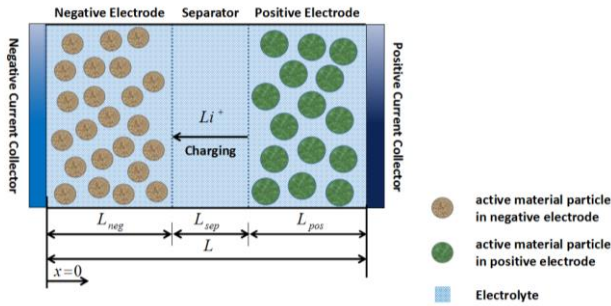
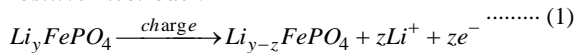


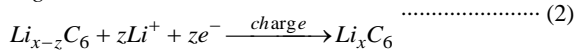
Fig.1. Electrochemical charging diagram of lithium-ion battery

During the charging process of the lithium-ion battery, the positive electrode material in the lithium-rich state undergoes oxidation reaction and loses electron-generated lithium ions. This part of lithium ions enters the electrolyte and diffuses through the separator to the negative electrode and electrolyte, and the electrons reach the negative electrode from the external circuit. During the charging process of the lithium-ion battery, the positive electrode material in the lithium-rich state undergoes oxidation reaction and loses electron-generated lithium ions [16-18]. This part of lithium ions enters the electrolyte and diffuses through the separator to the negative electrode electrolyte, and the electrons reach the negative electrode and the negative electrode from the external circuit. The lithium ion in the electrolyte undergoes a reduction reaction to form a solid lithium embedded in the negative electrode. Because the transmission speed of electrons in the external circuit is much larger than the movement speed of lithium ions in the electrolyte, this causes an imbalance in the ion concentration distribution inside the lithium ion battery to cause polarization phenomenon [19]. The equation for the above electrochemical process is as follows:

*Positive Electrode :*



*Negative Electrode :*



where x is the stoichiometric coefficient or the number of moles of lithium present in the graphite structure (C<sub>6</sub>), y is the stoichiometric coefficient or the number of moles of lithium in the olivine structure of iron phosphate (FePO<sub>4</sub>), Li<sup>+</sup> is the lithium-ion, z is the number of moles of lithium taking part in the electrochemical reaction.

## 2.2 Electrochemical Kinetics The Butler-Volmer equation

in electrode dynamics gives a calculation of the local reaction current density:

$$j_n = j_0 \left\{ \exp\left[\frac{\alpha_a F}{RT} \eta\right] - \exp\left[-\frac{\alpha_c F}{RT} \eta\right] \right\} \quad \dots\dots\dots (3)$$

where j<sub>0</sub> is the exchange current density, α<sub>a</sub> and α<sub>c</sub> are the charge transfer coefficients, F is the Faraday constant, R is the molar gas constant, T is the reaction thermodynamic temperature, η is the reaction overvoltage.

The exchange current density is given by

$$j_0 = Fk_0 c_l^{\alpha_a} (c_{s,max} - c_{s,surf})^{\alpha_a} c_{s,surf}^{\alpha_c} \quad \dots\dots\dots (4)$$

where k<sub>0</sub> is the reaction rate constant, c<sub>l</sub> is the electrolyte salt concentration, c<sub>s,max</sub> is the maximum lithium concentration in the active electrodes, c<sub>s,surf</sub> is the surface lithium concentration in the active electrodes.

The reaction overvoltage is given by

$$\eta = \phi_s - \phi_l - U_{eq} \quad \dots\dots\dots (5)$$

where φ<sub>s</sub> is the solid phase potential, where φ<sub>l</sub> is the liquid phase potential, U<sub>eq</sub> is the electrode equilibrium potential.

**2.3 Charge Conservation** The governing equation of charge conservation in electrode can be described as follows:

$$\nabla \cdot i_s + \nabla \cdot i_l = 0 \quad \nabla \cdot i_s = -S_a j_n \quad \nabla \cdot i_l = -S_a j_n \quad \dots\dots\dots (6)$$

where i<sub>s</sub> is the electronic current density in the electrode, i<sub>l</sub> is the ionic current density in the electrolyte, and S<sub>a</sub> is the specific surface area.

**2.3.1 Charge Conservation in Electrode** The transport of electrons in the electrode follows Ohm's law which can be expressed as follows:

$$i_s = -\sigma_s^{eff} \nabla \phi_s \quad \dots\dots\dots (7)$$

Where σ<sub>s</sub><sup>eff</sup> is the effective electrical conductivity of electrode.

**2.3.2 Charge Conservation in Electrolyte** The transport of lithium ions in electrolyte can be expressed as follows:

$$i_s = -\sigma_l^{eff} \nabla \phi_l + \frac{2RT\sigma_l^{eff}}{F} \left(1 + \frac{\partial \ln f_{\pm}}{\partial \ln c_l}\right) (1 - t_+) \nabla (\ln c_l) \quad \dots\dots\dots (8)$$

Where σ<sub>l</sub><sup>eff</sup> is the effective electrical conductivity of electrolyte, f<sub>±</sub> is the average molar activity coefficient, t<sub>+</sub> is the transferring number of lithium ions in electrolyte.

## 2.4 Mass Conservation

### 2.4.1 Lithium in Electrode Material Active Particles

The mass conservation of lithium in electrode material active particles can be described by Fick's law:

$$\frac{\partial c_s}{\partial t} + \frac{1}{r^2} \frac{\partial}{\partial r} \left( -r^2 D_s \frac{\partial c_s}{\partial r} \right) = 0 \quad \dots\dots\dots (9)$$

where  $c_s$  is the concentration of lithium in electrode material active particles,  $t$  is the time,  $r$  is the radial coordinate inside a spherical particle of electrode material,  $D_s$  diffusion coefficient of lithium in the active material.

#### 2.4.2 Lithium in Electrolyte

The mass conservation of lithium in electrolyte can be expressed as follows:

$$\varepsilon_l \frac{\partial c_l}{\partial t} + \nabla \cdot \mathbf{J}_l = \frac{S_a}{F} \quad (10)$$

$$\mathbf{J}_l = -D_l^{eff} \nabla c_l + \frac{i_l \cdot \mathbf{t}_+}{F} \quad (11)$$

where  $\varepsilon_l$  is the electrolyte volume fraction in the electrode,  $\mathbf{J}_l$  is the molar flux of lithium ions,  $D_l^{eff}$  is the effective diffusion coefficient of lithium ions in the electrolyte.

**2.5 Energy Conservation** Due to the different heat generation mechanism during charging and discharging, the heat of the lithium-ion battery is derived from reaction heat,  $Q_{rea}$ , ohmic heat,  $Q_{ohm}$ , activation polarization heat,  $Q_{act}$ . The energy conservation in the lithium-ion battery can be expressed as follows:

$$\rho C_p \frac{\partial T}{\partial t} - \lambda \nabla^2 T = Q_{rea} + Q_{act} + Q_{ohm} \quad (12)$$

where the  $\rho$  is the density,  $C_p$  is the heat capacity,  $\lambda$  is the thermal conductivity.

The reaction heat that due to electrochemical reaction can be expressed as follows:

$$Q_{rea} = S_a j_n T \frac{\partial U_{eq}}{\partial T} = S_a j_n T \frac{\Delta S}{F} \quad (13)$$

The ohmic heat that due to electrical ohmic losses in electrode and ionic losses electrolyte can be expressed as follows:

$$Q_{ohm} = -i_1 \cdot \nabla \phi_1 - i_2 \cdot \nabla \phi_2 \quad (14)$$

The activation polarization heat that due to electrochemical reaction polarization between the particle surface of the active material and the electrolyte can be expressed as follows:

$$Q_{act} = S_a j_n \eta \quad (15)$$

#### 2.6 Diffusion Polarization Electrolyte of Positive Electrode

According to the different generation mechanism, the charge and discharge polarization of lithium-ion batteries is divided into ohmic polarization, electrochemical polarization and concentration polarization [20]. The polarization phenomenon is closely related to the ambient temperature of the lithium-ion battery, the charge and discharge current, and the battery SOC [21-23]. Lithium-ion batteries belong to the electrochemical product so the generation of polarization voltage appears with charge and discharge and this phenomenon can not be eliminated. This paper focuses on the low temperature characteristics of the diffusion polarization electrolyte of the positive electrode. The average polarization voltage is as follows [7]:

$$P_v = -\frac{1}{J_t} \int \frac{2RT}{c_l F} \kappa_c \frac{\partial c_l}{\partial x} J_l dx \quad (16)$$

where the  $J_t$  is the total current per cross-sectional area,  $\kappa_c$  is the concentration conductivity.

The total current per cross-sectional area can be expressed as follows:

$$J_t = \int S_a j_n dx \quad (17)$$

**2.7 Model Validation** In order to verify the validity of the model, a Chinese manufacturer's LR1865EC lithium-ion battery (nominal voltage 3.2V, nominal capacity 1.3Ah, charge cut-off voltage 3.6V) was used as the test sample, and the Arbin-LBT battery test system and The temperature box is the test platform. The test samples are subjected to 1C constant current charging test under the three low temperature conditions of  $-5^\circ\text{C}$ ,  $-10^\circ\text{C}$  and  $-15^\circ\text{C}$  respectively. The structure of the test platform is shown in the Figure 2.

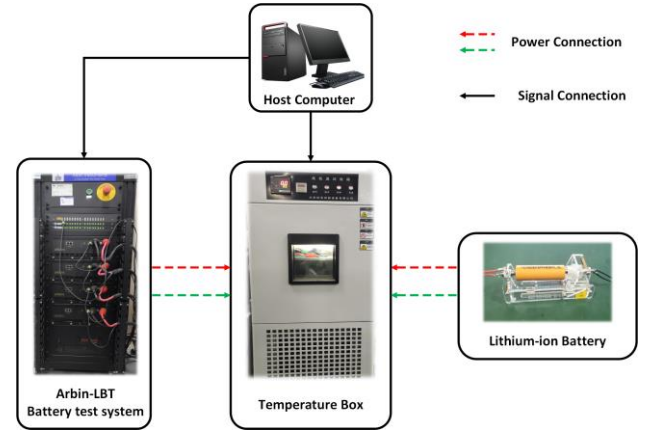


Fig. 2. Experimental setup of charging system in low temperature.

In the state of full battery, the commercial lithium-ion battery is surrounded by an outer protective shell, which is a very closed system. The data of the positive electrode, the separator, the negative electrode is difficult to collect. Therefore, in this paper, the validity of the model is verified from the side by comparing

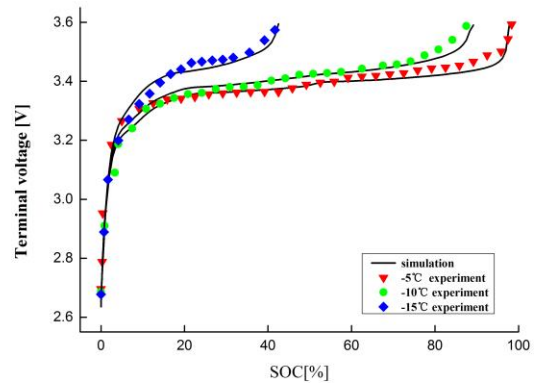


Fig. 3.  $-5^\circ\text{C}$ ,  $-10^\circ\text{C}$ ,  $-15^\circ\text{C}$ , 1C charge validations.

the experimental and simulated values of the charging terminal voltage curve of the lithium-ion battery [24,25]. At the same temperature, a total of 4 samples are tested simultaneously, and the average voltage of the four samples is taken at the same time. Figure 3 is a comparison of the test results and simulation results of the 1C constant current charging terminal voltage in three low temperature environments. It can be seen that the simulated values and experimental values are consistent at three temperatures, indicating that the model has good accuracy.

### 3. Results

**3.1 Diffusion Polarization Voltage of Positive Electrode in Electrolyte** Figure 4 shows the variation of diffusion polarization voltage of positive electrode in electrolyte with the overall SOC of the battery in three low temperature environments. It can be seen from the figure that the diffusion polarization voltage in electrolyte is divided into three stages: initial period, plateau period and rising period. These three stages together constitute a basic trend of rising first, then stabilizing and finally rising again, and the temperature decrease does not affect the trend of this polarization voltage, which indicates that diffusion polarization voltage of positive electrode in electrolyte is independent of the SOC of lithium-ion battery but is related to the charging process.

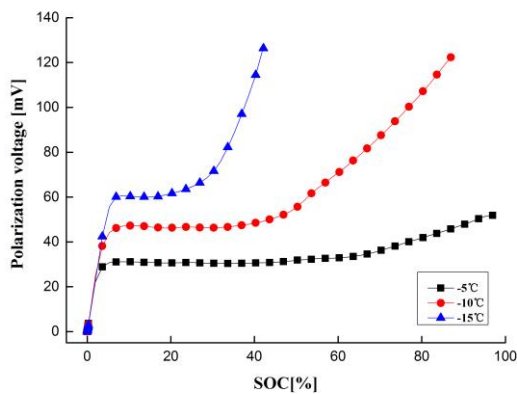


Fig. 4. -5°C, -10°C, -15°C, 1C charge validations.

The variables SOC<sub>1</sub>, SOC<sub>2</sub>, and SOC<sub>3</sub> are set to represent the initial battery SOC during the plateau period, the initial battery SOC and the charge end SOC of the rising period of diffusion polarization voltage of positive electrode in electrolyte, respectively; the variables V<sub>pp\_ave</sub> and V<sub>pr\_max</sub> are set to represent average polarization voltage value during the plateau period and the maximum polarization voltage value during the rise period, respectively. Table 1 shows the values of each variable under three low temperature conditions.

Table 1. Variable value table in polarization voltage curve.

Temperature	SOC <sub>1</sub>	SOC <sub>2</sub>	SOC <sub>3</sub>	V <sub>pp_ave</sub>	V <sub>pr_max</sub>
-5°C	5.28%	66.94%	96.94%	31.39 mV	51.85 mV
-10°C	5.28%	50.28%	86.94%	47.82 mV	122.37 mV
-15°C	6.94%	20.28%	42.14%	60.48 mV	126.35 mV

It can be seen from Table 4 that the decrease of the ambient temperature in the initial period will not affect the value of SOC<sub>1</sub>, and this variable will only increase slightly at -15°C. As the temperature decreases, average value of the polarization voltage during the plateau period V<sub>pp\_ave</sub> will gradually increase. The SOC interval of the platform period is gradually shortened, it can be seen the SOC interval width of the -15°C in the platform period is only 21.63% at -5°C, while the average value of the polarization voltage V<sub>pp\_ave</sub> is 192.67% at -5°C. The polarization voltage will be significantly different in the three ambient temperatures during the rising period, the slowest rise and the minimum peak value of the polarization voltage appear at -5°C, the fastest rise and the maximum peak value of polarization voltage appear at -15°C, which indicates the lower temperature at this stage, the faster the polarization voltage changes, and the more severe the degree of diffusion polarization voltage of positive electrode in electrolyte.

The above variables can well explain the change about diffusion polarization voltage of positive electrode in electrolyte. In this paper, the dimensionless function P<sub>dpe</sub> is used to characterize the degree of this kind polarization at low temperature. Its definition is as follows.

$$P_{dpe} = \frac{V_{pp\_ave}}{SOC_2 - SOC_1} \frac{V_{pr\_max} - V_{pp\_ave}}{SOC_3 - SOC_2} \dots\dots\dots (16)$$

It can be seen from the values in the Table 2 that the temperature decrease will enhance the diffusion polarization voltage of positive electrode in electrolyte, Especially when it reaches -15°C, this phenomenon will increase significantly. When the ambient temperature is -10°C and -5°C, the value is 2.49% and 15.81% of the value at -15°C, respectively.

Table 2. Variable value table in polarization voltage curve.

Temperature	-5°C	-10°C	-15°C
P <sub>dpe</sub>	0.34	2.16	13.66

### 3.2 Analysis of Positive Electrolyte Salt Concentration Gradient

The main cause of diffusion polarization in electrolyte is the accumulation of lithium-ion concentration gradient in the electrolyte, and the main manifestation of this accumulation is the time-space distribution of the positive electrolyte salt concentration.

During charging, charge transferring and generation of a large amount of lithium ions occur simultaneously in the oxidation reaction of the positive electrode material. These lithium ions move toward the separator under the interaction of electric field force and concentration gradient, but the movement speed of lithium ions is relatively slow and the porous electrode material has a certain thickness, lithium-ions near the side of separator will preferentially enter the separator, and lithium ions near the side of the current collector will lag behind, which caused the phenomenon that the electrolyte salt concentration near the collector side will be higher than the side close to the separator in the positive porous electrode and the concentration gradient is thus formed. The decrease in temperature has a negative effect on the conductivity, activity dependence and diffusion coefficient of the electrolyte. Macroscopically, the viscosity of the electrolyte

increases, which makes the diffusion of ions slower and the diffusion polarization of positive electrode in electrolyte is more serious.

Figure 5, Figure 6 and Figure 7 show the change of electrolyte salt concentration with time in the thickness direction of the positive electrode under three low temperature conditions respectively. The conclusions we can draw are as follows.

(1) The electrolyte salt concentration in three low temperature environments has a process of first rising, then stabilizing, and finally rising again during charging progress. This is because the addition of lithium ions at the initial stage of charging causes a rapid increase in the initial concentration of the electrolyte. During the middle of charging, the generation and diffusion of lithium ions will balance the electrolyte salt concentration. However, as the degree of charging increases, the ability of the negative electrode to receive lithium ions decreases, and the salt concentration in the negative pore electrode increases, which cause the decreasing of concentration gradient in the lithium ion battery as a whole, the reduction of diffusion effect in positive electrolyte and the accumulation of lithium ions in the positive electrode. As a result, the concentration of the positive electrolyte salt finally rises once. It can be seen from the following three figures that the gradual decrease in temperature causes the liquid phase diffusion ability of lithium ions in positive to decrease, resulting in an overall rise of electrolyte concentration in the middle and late charging stages.

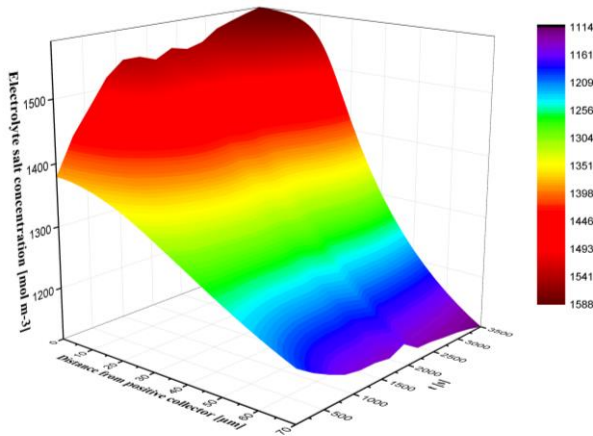


Fig. 5. Time and space distribution of electrolyte salt concentration at -5°C.

(2) Time accumulation of electrolyte salt concentration: the overall level of electrolyte salt concentration under three low temperature conditions has greatly improved with time. It can be seen from Figure 5 that the electrolytic salt concentration will not exceed 1600 mol/m<sup>3</sup> during the entire charging process at -5°C, but the electrolytic salt concentration within 150 s will reach or exceed this in the low temperature conditions of -10°C and -15°C, which can be seen from Figure 6 and Figure 7. This is due to the influence of low temperature on the diffusion coefficient and other parameters of positive electrolyte. As the charge progresses, the positive electrode continuously generates lithium ions by the charge transfer of the oxidation reaction, but as the temperature decreases, the parameters such as the liquid phase diffusion coefficient are continuously reduced. The generated lithium ions cannot be moved to the side close to the separator in time, so that the electrolyte salt concentration is increased as a whole.

(3) Spatial accumulation of electrolyte salt concentration: Since the continuously generated lithium ions cannot diffuse to the side of separator in time, as the temperature decreases, lithium ions will accumulate to a certain extent at the side of the current collector, which is evident in Figure 7. It can be seen from Figure 7 that a stable concentration appears near the end of the current collector at 600s, and as the charge progresses, this concentration increases in the thickness direction of the electrode to cause an electrolyte salt concentration platform which is also a certain manifestation in Figure 6. This indicates that under certain low temperature conditions, the lithium ions near the side of the current collector appear to diffusion stagnation. The phenomenon that the lithium ions are continuously generated but cannot be time-shifted greatly aggravates the diffusion polarization of positive electrode in electrolyte at low-temperature charging progress.

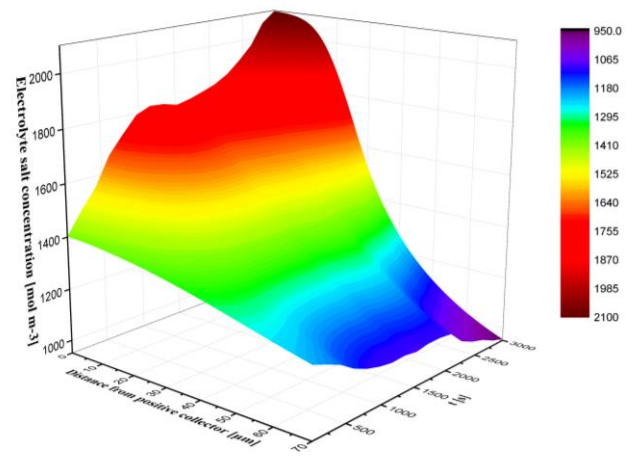


Fig. 6. Time and space distribution of electrolyte salt concentration at -10°C

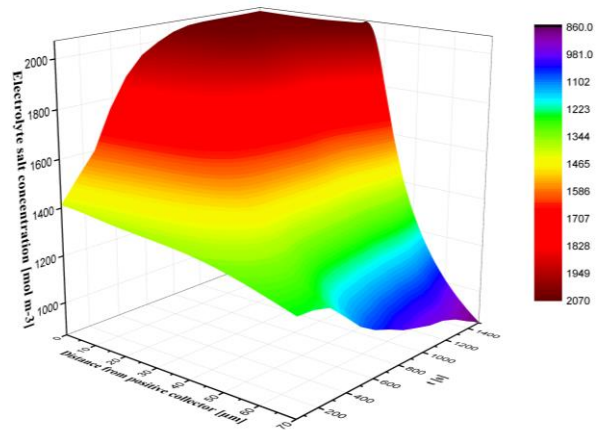


Fig. 7. Time and space distribution of electrolyte salt concentration at -15°C

**3.3 Analysis of Positive Electrolyte Current Density** The current in the external circuit comes from the movement of electrons and the current in the electrolyte comes from the movement of lithium ions. The electrolyte salt concentration can only indicate the instantaneous distribution of lithium ions in the electrolyte and the electrolyte current density can indicate the rate

of movement of lithium ions in the electrolyte. The electrolyte salt concentration can only indicate the instantaneous distribution of lithium ions in the electrolyte and the electrolyte current density can indicate the rate of movement of lithium ions. This explains the accumulation of lithium ion concentration gradients in the electrolyte from another perspective, and also explains the diffusion polarization of positive electrode in electrolyte.

Figure 8 shows the distribution of electrolyte current density in the thickness direction of the positive electrode under three low temperature conditions at 300s. The positive electrode current density generally shows a tendency to grow from the current collector to the separator in the thickness direction, and the initial value and the peak value are consistent. This is because the positive electrode generates lithium ions simultaneously in the thickness direction while charging in the one-dimensional electrochemical model, but these lithium ions move toward one end of the separator. The greater the lithium ion flux near the end of the membrane, the greater the corresponding electrolyte current density, reaching a maximum at the junction where the positive electrode is connected to the separator.

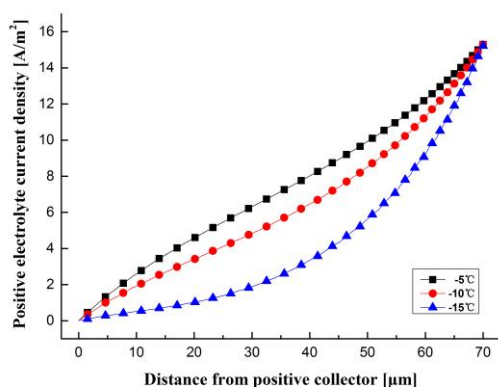


Fig. 8. Positive electrolyte current density at 300s

Figure 8 shows the distribution of electrolyte current density in the thickness direction of the positive electrode under three low temperature conditions at 300 s.

At 300s, the decrease in temperature will cause the current density of the positive electrolyte to decrease, resulting in the lowest electrode current density at the same thickness of the positive electrode at  $-15^{\circ}\text{C}$ , the highest at  $-5^{\circ}\text{C}$ . And this gap is the largest at the midpoint of the positive electrode thickness. On the other hand, the gradual decrease in temperature causes a certain increase in the growth rate of the electrolyte current density. From Figure 8, it can be seen that the electrolyte current density increases fastest at  $-15^{\circ}\text{C}$ . This is because the decrease in temperature increases the viscosity of the electrolyte, which causes the movement speed of lithium ions to be slower at the same thickness, so that the corresponding current density decreases as the temperature decreases. However, the decrease in temperature also aggravates the accumulation of lithium ion concentration in the liquid phase, so that the absolute value of the lithium ion flux on the adjacent back end unit is large, so that the lower the temperature, the faster the current density of the positive electrolyte increases. However, the decrease in temperature also aggravates the accumulation of lithium ion concentration in the liquid phase, so that the absolute value of the lithium ion flux on

the adjacent thickness unit is relatively large. Thus, the lower the temperature, the faster the current density of the positive electrode electrolyte grows.

Figure 9 is a distribution diagram of the current density of the positive electrode electrolyte. Under the three low temperature conditions, a certain current density platform appears in the positive electrolyte during charging, wherein the  $-5^{\circ}\text{C}$  and  $-10^{\circ}\text{C}$  corresponding platforms appear in the part near the separator, and the platform height is consistent with the maximum current density; and the  $-15^{\circ}\text{C}$  corresponding platform appears near the current collector, and the platform is close to zero.

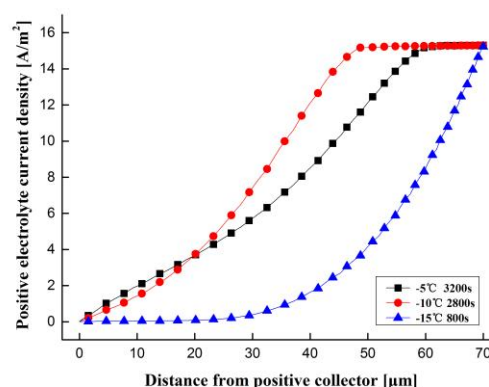


Fig. 9. Positive electrolyte current density at the end of charging

This is because the increase in electrolyte viscosity caused by the decrease of temperature has a cumulative phenomenon of electrolyte salt concentration. The above curve shows that the accumulation of  $-5^{\circ}\text{C}$  and  $-10^{\circ}\text{C}$  appears on the side close to the separator because the current density at the intersection of the separator and the electrode is constant but the accumulated lithium ion concentration near the side of the separator exceeds the requirement corresponding to the maximum current density, and the positive current has a maximum current density within a certain width near the side of the separator. At  $-15^{\circ}\text{C}$ , the electrolyte viscosity is further increased due to further decrease in temperature, and a large amount of lithium ions generated by the oxidation reaction on the side close to the current collector cannot be actively transported to the side of the separator, and the retention of lithium ions causes the electrolyte current density to be almost zero. The phenomenon, which at the same time corresponds to the electrolyte concentration platform in Figure 7.

**4 Conclusions** In this paper, the electrochemical-thermal model was used to study the variation of the diffusion polarization electrolyte of positive electrode in the low-temperature conditions under the constant-current charging process, and the degree of this polarization was characterized by the variable  $P_{dpe}$ , and the cause of this polarization change was analyzed further by the electrolyte salt concentration and electrolyte current density. The conclusion is as follows.

(1) The low temperature condition increases the diffusion polarization electrolyte of positive electrode in the process during constant current charging of lithium ion battery to a certain extent, and the lower the temperature, the greater the degree of influence.

(2) The spatial and temporal distribution of electrolyte salt concentration and electrolyte current density in the thickness

direction of the electrode explains the effect of the accumulation of concentration gradient on diffusion polarization of positive electrode in electrolyte from another point of view.

### Acknowledgement

This research was financially supported by Natural Science Foundation of Hebei Province (E2016202206).

### References

- (1) Meng X, Zhang Z, Xia, et al. Two-dimensional electrochemical - thermal coupled modeling of cylindrical LiFePO<sub>4</sub> batteries. *Journal of Power Sources*. 2014, 256, 233-243.
- (2) Jie L, Yun C, et al. 3D simulation on the internal distributed properties of lithium-ion battery with planar tabbed configuration. *Journal of Power Sources*. 2015, 293, 993-1005.
- (3) Yilmaz M, Krein P.T. Review of battery charger topologies, charging power. *Transactions on Power Electronics*, 2013, 28(5), 2151-2169.
- (4) Zhang S.S, Xu K, Jow T.R. A new approach toward improved low temperature performance of li-ion battery. *Electrochemistry Communications*. 2002, 4(11), 928-932.
- (5) Wang T, Wu X, et al. Performance of plug-in hybrid electric vehicle under low temperature condition and economy analysis of battery pre-heating. *Journal of Power Sources*. 2018, 401, 245-354.
- (6) Feng G, Li Z, et al. Polypropylene/hydrophobic-silica-aerogel-composite separator induced enhanced safety and low polarization for lithium-ion batteries. *Journal of Power Sources*. 2018, 376, 177-183.
- (7) Bo Y, Lim C, et al. Analysis of polarization in realistic li ion battery electrode microstructure using numerical simulation. *Electrochimica Acta*. 2015, 185, 125-141.
- (8) Yu W, Zhengyu C, et al. Overcharge durability of Li<sub>4</sub>Ti<sub>5</sub>O<sub>12</sub> based lithium-ion batteries at low temperature. *Journal of Energy Storage*, 2018, 19, 302-310.
- (9) Nyman A, Zavalis, T.G, et al. Analysis of the polarization in a Li-ion battery cell by numerical simulations. *Journal of the Electrochemical Society*, 2010, 157, 1236-1246.
- (10) Meng X, Choe S.Y. Dynamic modeling and analysis of a pouch type LiMn<sub>2</sub>O<sub>4</sub>/carbon high power li-polymer battery based on electrochemical-thermal principles. *Journal of Power Sources*, 2012, 218, 357-367.
- (11) Amiribavandpour P, Shen W, et al. An improved theoretical electrochemical-thermal modelling of lithium-ion battery packs in electric vehicles. *Journal of Power Sources*, 2015, 284, 328-338.
- (12) Han X, Ouyang M, et al. A comparative study of commercial lithium ion battery cycle life in electrical vehicle: aging mechanism identification. *Journal of Power Sources*, 2014, 251(2), 38-54.
- (13) Krieger E.M, Cannarella J, Arnold C.B. A comparison of lead-acid and lithium-based battery behavior and capacity fade in off-grid renewable charging applications. *Energy*, 2013, 60(4), 492-500.
- (14) Li J, Wang L, et al. New method for parameter estimation of an electrochemical-thermal coupling model for LiCO<sub>2</sub> battery. *Journal of Power Sources*, 2016, 307, 220-230.
- (15) Bahiraei F, Fartaj A, Nazri, G.A. Electrochemical-thermal modeling to evaluate active thermal management of a lithium-ion battery module. *Electrochimica Acta*, 2017, 254, 59-71.
- (16) Wu X, Viswanathan V.V, et al. Investigation on the charging process of Li<sub>2</sub>O<sub>2</sub>-based air electrodes in Li-O<sub>2</sub> batteries with organic carbonate electrolytes. *Journal of Power Sources*, 2011, 196, 3894-3899.
- (17) Guo S, Li H, et al. Numerical simulation study on optimizing charging process of the direct contact mobilized thermal energy storage. *Applied Energy*, 2013, 112, 1416-1423.
- (18) Xue X, Wang S, et al. Hybridizing energy conversion and storage in a mechanical-to-electrochemical process for self-charging power cell. *Nano Letters*, 2012, 12(9), 5048-5054.
- (19) Jie L, Yun C, et al. An electrochemical - thermal model based on dynamic responses for lithium iron phosphate battery. *Journal of Power Sources*, 2014, 255(6), 130-143.
- (20) Yang S, Deng C, et al. State of Charge Estimation for Lithium-Ion Battery with a Temperature-Compensated Model. *Energies*, 2017, 10(10), 1560.
- (21) Jiang J, Liu Q, et al. Evaluation of acceptable charging current of power Li-Ion batteries based on polarization characteristics. *IEEE Transactions on Industrial Electronics*, 2014, 61(12), 6844-6851.
- (22) Noelle D.J, Meng W, et al. Internal resistance and polarization dynamics of lithium-ion batteries upon internal shorting. *Applied Energy*, 2018, 212,

796-808.

- (23) Bazak J.D, Krachkovskiy S.A, Goward G.R. Multi-temperature in situ magnetic resonance imaging of polarization and salt precipitation in lithium-ion battery electrolytes. *Journal of Physical Chemistry C*, 2017, 121(38).
- (24) Severin L.H, Mathias S, et al. Quantitative validation of calendar aging models for lithium-ion batteries. *Journal of Power Sources*, 2018, 400, 402-414
- (25) Ye Y, Shi Y, et al. Electro-thermal modeling and experimental validation for lithium ion battery. *Journal of Power Sources*, 2012, 199(1), 227-238.

### Nomenclature

#### List of Symbols

x	Distance in porous electrode(m)
r	Particle radius(m)
L	thickness of battery component(m)
$j_n$	Local reaction current density(A m <sup>-2</sup> )
$j_0$	Exchange current density(A m <sup>-2</sup> )
$j_t$	Total current per cross-sectional area(A m <sup>-2</sup> )
T	Reaction thermodynamic temperature(K)
$k_0$	Reaction rate constant
$c_s$	Concentration of lithium in electrode material active particles(mol m <sup>-3</sup> )
$c_l$	Electrolyte salt concentration(mol m <sup>-3</sup> )
$D_s$	Diffusion coefficient of electrode
$D_l$	Diffusion coefficient of electrolyte
k	thermal conductivity (W (m K) <sup>-1</sup> )
SOC	State of charge
$Q_{rea}$	Reaction heat(W m <sup>-3</sup> )
$Q_{ohm}$	Ohmic heat(W m <sup>-3</sup> )
$Q_{act}$	Activation polarization heat(W m <sup>-3</sup> )

#### Greek

$\eta$	Over potential(V)
$\alpha_a$	Transfer coefficient in positive electrode
$\alpha_c$	Transfer coefficient in negative electrode
$\phi_s$	Solid phase potential(V)
$\phi_l$	Liquid phase potential(V)
$\sigma_s$	Electronic conductivity of electrode(S m <sup>-1</sup> )
$\sigma_l$	Ionic conductivity of electrolyte (S m <sup>-1</sup> )
$\epsilon_s$	Active material volume fraction
$\epsilon_l$	Electrolyte volume fraction
$\kappa_c$	Concentration conductivity

#### Subscripts and Superscripts

neg	Negative electrode
sep	Separator
pos	Positive electrode
s	Solid phase
l	Liquid phase
t	Tota
eff	Effective value
surf	Surface of active material particle





$E_{s,k}$	$\text{kJ mol}^{-1}$	30	-	20
$\sigma_s$	$\text{S m}^{-1}$	100		0.1
$D_l$		-	Table A1	-
$k_l$		-	Table A1	-
$v$		-	Table A1	-
$t_+$		-	Table A1	-
$\sigma_1$		-	Table A1	-
$k$	$\text{W m}^{-1} \text{K}^{-1}$	1.04	1	1.48
$\rho$	$\text{Kg m}^{-3}$	2660	492	1500
$cp,s$	$\text{J kg}^{-1} \text{K}^{-1}$	1437	700	1260
$cp,l$	$\text{J kg}^{-1} \text{K}^{-1}$		2055	
$T_{\text{ref}}$	$\text{K}$		273.15	
$F$	$\text{C mol}^{-1}$		96487	